Communication

Not peer-reviewed version

A Wideband Circularly Polarized Dipole Antenna with Compact Size and Low-Pass Filtering Response

Xianjing Lin , Zhang Run Weng , Yi Bin Hong , Yao Zhang *

Posted Date: 23 May 2024

doi: 10.20944/preprints202405.1496.v1

Keywords: Wideband antenna; cross dipole antenna; circularly polarized antenna; filtering antenna

Article

A Wideband Circularly Polarized Dipole Antenna with Compact Size and Low-Pass Filtering Response

Xianjing Lin [1], Zhang Run Weng [1], Yi Bin Hong [1], Yao Zhang [2,*]

[1] School of Electronic Engineering and Intelligence, Dongguan University of Technology, Dongguan, Guangdong 523808, China;
[2] Institute of Electromagnetics and Acoustics, Xiamen University, Xiamen, Fujian 361005, China
[*] Correspondence: zhangsantu@xmu.edu.cn(Y.Z.)

Abstract: This paper presents a compact wideband circularly polarized cross dipole antenna with low-pass filter response. It consists of two pairs of folded crossed dipole arms printed separately on both sides of the top substrate, and the two dipole arms on the same surface are connected by an annular phase-shifting delay line to generate circular polarization. A bent metal square ring and four small metal square rings around the cross dipoles are employed to introduce new resonant frequencies, effectively extending the impedance and axial ratio bandwidth. Four square patches printed on the middle substrate are connected to the ground plane by the vertical metal plates, in order to reduce the antenna height. Thus, a compact wideband circularly polarized antenna is realized. In addition, a transmission zero can be introduced at the upper frequency stopband by the bent metal square rings, without using extra filter circuits. For verification, the proposed model is implemented and tested. The overall size of the model is 90mm $\times$ 90mm $\times$ 33mm($0.37\lambda_0 \times 0.37\lambda_0 \times 0.14\lambda_0$, λ_0 denotes the center operating frequency). The measured impedance bandwidth and 3 dB axial ratio bandwidth are 53.3% and 41%, respectively. More than 15 dB upper-band radiation suppression level is realized, indicating a good low-pass filter response.

Keywords: wideband antenna; cross dipole antenna; circularly polarized antenna; filtering antenna

---

1. Introduction

Compared to linearly polarized antennas, circularly polarized antennas can receive arbitrarily polarized incoming waves and therefore they are widely used in wireless communication, radar, radio frequency identification and satellite communication systems [1].

Cross-dipole antennas have been widely studied for their ability to achieve good circular polarization [2–24]. The traditional cross dipole circular polarization antenna is connected by two annular delay line phase shifters to the four narrow arms of the cross dipole and fed through the coaxial line, which can achieve a 3 dB axial ratio bandwidth of about 7% [2,3]. In order to broaden the axial ratio bandwidth, the crossed dipole arms can be changed into wide rectangular [4], wide ring [5], bowtie [6], and the divided wide dipole arms [7]. Or, using the folded microstrip lines instead of annular delay line phase shifters [8], or parasitic units [9–11] around the dipole arms, the axial ratio bandwidth can be expanded to 25%-90%. However, for these designs, wide axial ratio bandwidth is usually obtained with increasing antenna size or height, or unstable radiation patterns. In order to reduce the antenna size, the most direct way is to fold the cross-dipole arms [12–18] or the feed network [19], but this results in limited axial ratio bandwidth (7%-13%). Using coupled slips instead of annular delay line phase shifters and loading stepped square rings can effectively reduce the plane size and maintain a wide axial ratio bandwidth [20], but the antenna height is stable at 0.25 λ_0. The antenna height can be reduced from 0.25 λ_0 to around 0.16 λ_0 by loading a short-circuited wall at the radiation patch [21], or using SIW feed network [22] and AMC reflectors [23,24]. However, these methods can result in large plane sizes or high cross-polarized radiation, which leads to the radiation pattern deterioration. For cross-dipole circularly polarized antennas, it is still challenging to realize a compact structure while maintaining wide axial ratio bandwidth and stable in-band radiation pattern.

In this work, by folding narrow cross dipole arms and introducing a bent square ring and four small metal square rings around the dipole arms, the plane size of the antenna can be effectively reduced, and 41% of the axial ratio bandwidth can be obtained. Then, the profile height can be reduced to 0.14 λ_0 by introducing four patches connected by the metal plates around its outer right-angle edges to the ground plane. In addition, the bending metal square ring can not only widen the axial ratio bandwidth but also introduce a radiation zero at the high frequency stopband, achieving a good low-pass filtering response.

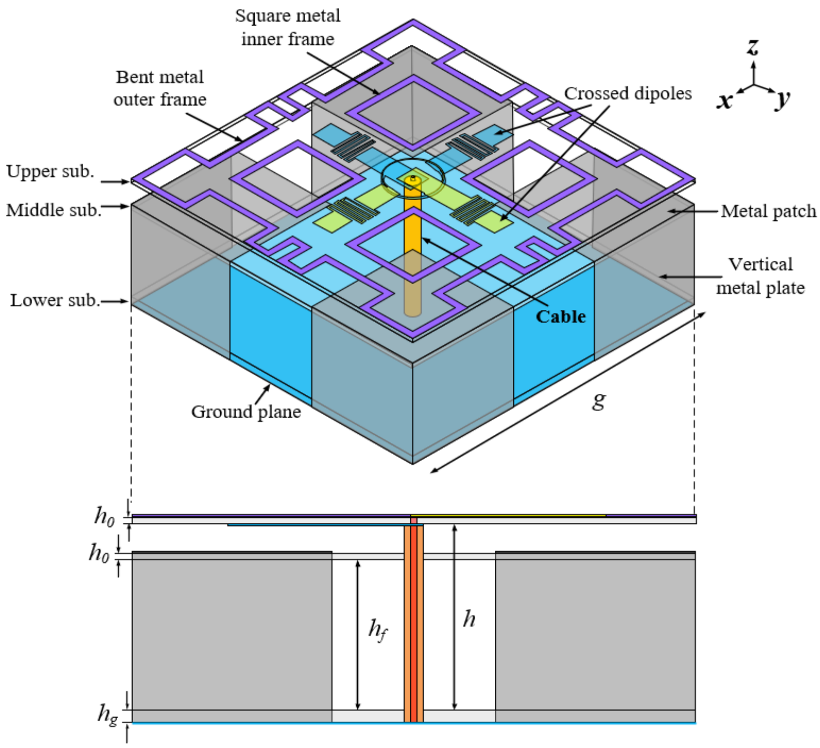

(a)

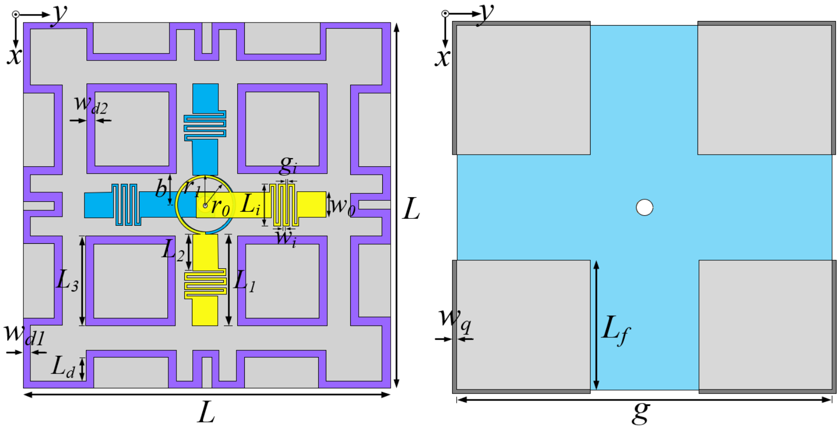

(b) (c)

Figure 1. Antenna structure, (a) total view, (b) dipole antenna layer top side and (c) middle dielectric layer top side.($g = 90, L = 90, L_1 = 22, L_2 = 16, L_3 = 22, L_f = 32, w_0 = 6, L_i = 10, w_i = 0.5, g_i = 0.6, r_0 = 6.9, r_1 = 7.1, b = 7.5, w_{d1} = 1.8, w_{d2} = 2, L_d = 6, h = 30, h_f = 25, h_0 = 1, h_g = 2$, all in mm).

 doi:10.20944/preprints202405.1496.v1

2. Antenna Structure and Design Procedure

2.1. Antenna Structure

The structure of the proposed compact wideband circularly polarized cross dipole antenna with low-pass filter response is shown in Figure 1. It consists of two folded cross dipoles, a bent metal outer square ring, four metal inner square rings, four square metal patches, and four vertically grounded metal plates. The antenna is fed by coaxial cables. The folded cross dipole arms are printed separately on both sides of the top substrate, and a bent metal outer square ring and four-square metal inner square rings are printed around the dipole arms on the upper surface. Four square patches are printed on the upper surface of the middle substrate, and four vertical metal plates are connected at the outer right angles of the four-square patches. A metal ground plane is printed on the lower surface of the bottom substrate, the coaxial inner conductor is connected to the dipole arm printed on the upper surface of the top substrate, and the outer conductor is connected to the dipole arm printed on the back side. The FR4 epoxy substrate ($\varepsilon_r = 4.4$, tanδ = 0.02) of height 1 mm is used for the design.

2.2. Design Procedure

To reveal the working principle of the proposed antenna, Figure 2 shows five reference antennas and corresponding S-parameter and axial ratio results. As seen in Figure 2(a), it is a folded cross dipole arms CP antenna structure. The S-parameter and AR values are also illustrated in Figure 2(a). It can be seen that the -10 dB impedance band ranges from 1.25 to 1.49 GHz (17.5%), with only one CP resonant frequency in the passband, and the 3dB axial ratio bandwidth (5.1%) is very limited. When a large square ring is loaded at the periphery of the cross-dipole arms, the overall operation frequency band is shifted to the lower band, and the impedance bandwidth is extended to 39.66% (0.95 GHz-1.42 GHz). Meanwhile, two CP resonant frequencies in the passband are emerged, but the circular polarization performances are not good, as seen in Figure 2(b). To improve the circular polarization performance, four metal square rings are introduced between the large square ring and the cross dipole, as observed in Figure 2(c). In this case, the plane size and antenna height are very large. Then the reference Antennas IV and V have been developed. By adding a middle substrate right under the cross dipole, and printing four square patches at the upper surface of the substrate, then connecting the patches to four vertically grounded metal plates, the profile height of the antenna can be effectively reduced with the performance nearly unchanged. Figure 2(d) shows the structure of the reference Antenna IV and its results. To further reduce the plane size of the antenna, the large square ring is bent, and the performance is still unchanged, as illustrated in Figure 2(e). Hereto, the compact wideband CP cross dipole antenna is realized. Figure 3 shows the current distributions at the two CP resonant frequencies of 1.12 GHz and 1.44 GHz when phase = 0° and 90°. As observed, the antenna operates as a LHCP antenna.

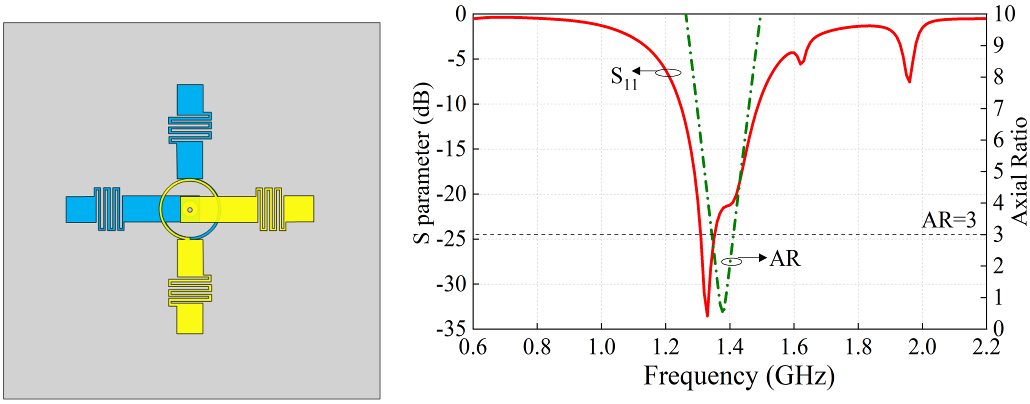

(a) Original Antenna I and results

Preprints.org (www.preprints.org) | NOT PEER-REVIEWED | Posted: 23 May 2024 doi:10.20944/preprints202405.1496.v1

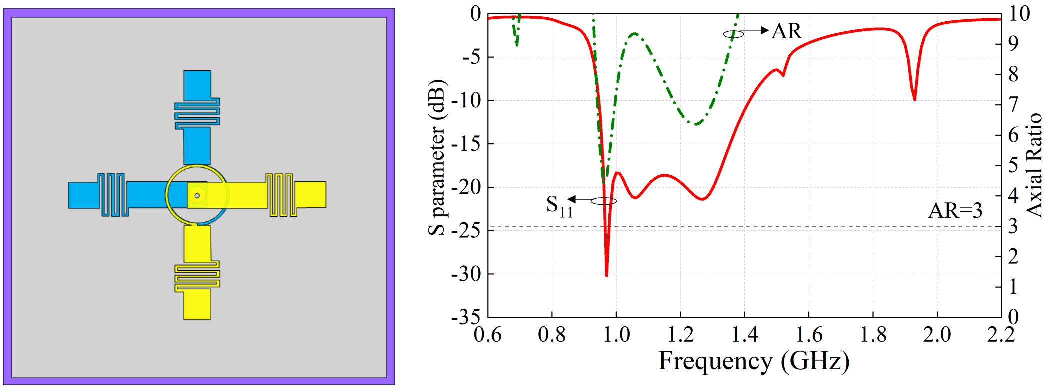

(b) Reference Antenna II and results

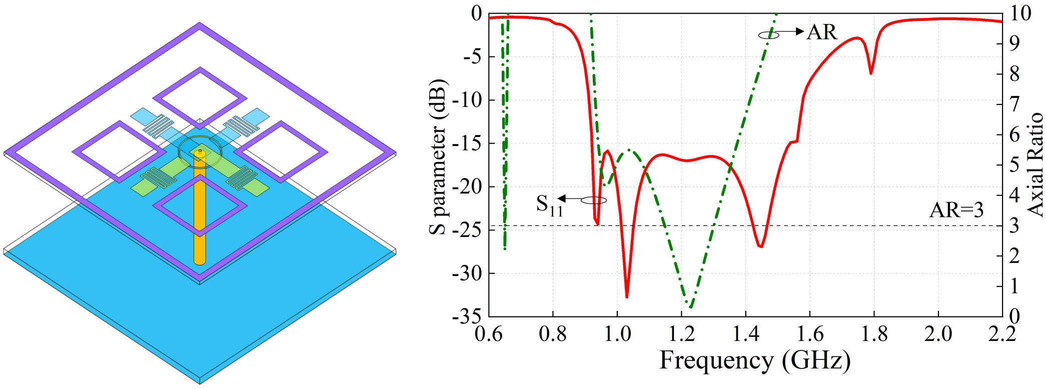

(c) Reference Antenna III and results

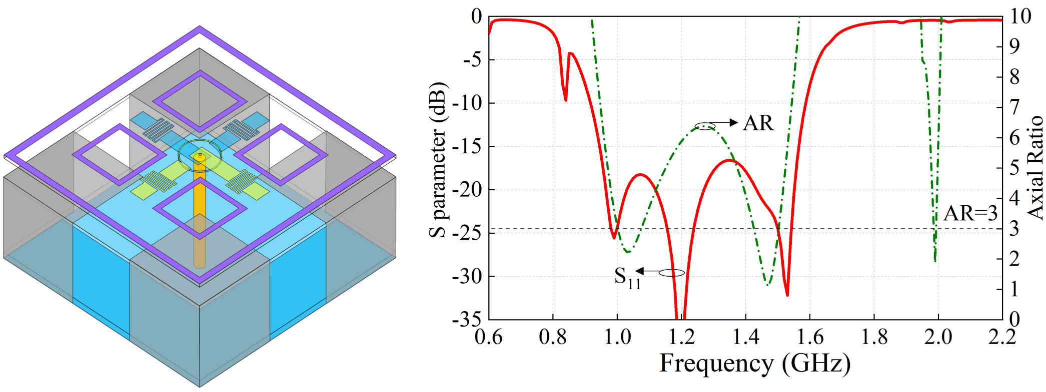

(d) Reference Antenna IV and results

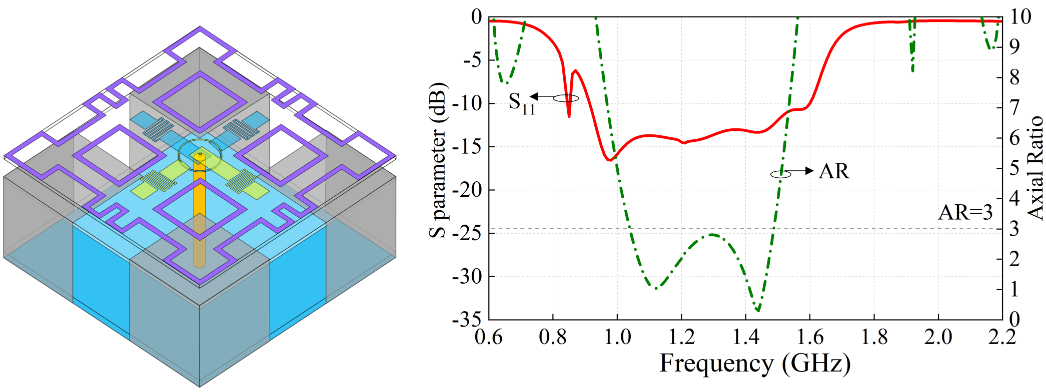

(e) Reference Antenna V and results

Figure 2. Structure and results of five antennas.

Preprints.org (www.preprints.org) | NOT PEER-REVIEWED | Posted: 23 May 2024 doi:10.20944/preprints202405.1496.v1

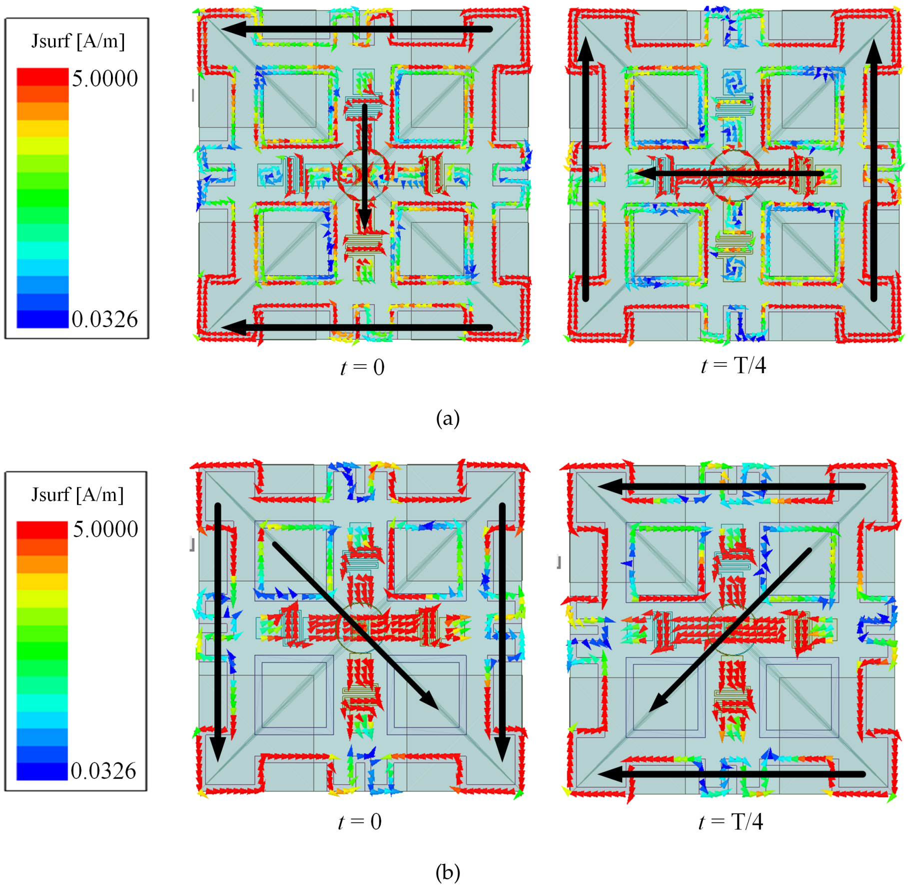

Figure 3. Surface current distribution of the reference Antenna V when the phase is 0° and 90° at operating frequency (a) 1.12 GHz and (b) 1.44 GHz.

2.3. Low-Pass Filtering Radiation Response

The antenna realized gain against the ring parameters L and L_1 are illustrated in Figure 4. Low-pass type radiation response is seen with two controllable upper-band radiation nulls. As presented in Figure 4(a), the upper-band radiation $Null_1$ frequency increases from about 1.62 GHz to 1.82 GHz when L (the length of the bent square ring) deceases from 100 mm to 85 mm, while the upper-band radiation $Null_2$ frequency is nearly fixed. Similar phenomenon can be seen when the folded cross dipole arm L_1 changes. Both of the two nulls are introduced at the upper-band, which make the proposed antenna have a good low-pass filtering response.

To reveal the working principle of the low-pass filtering radiation response, the antenna surface current distribution at the two radiation nulls of 1.78 GHz and 1.92 GHz are shown in Figure 5. It's observed in Figure 5(a) that at the $Null_1$ frequency 1.78 GHz, the surface currents mainly concentrate on the bent mental square ring, the currents flow in opposite directions at the horizontal and vertical direction of the square ring. Thus, it does not effectively radiate. With regard to the radiation $Null_2$, the currents mainly concentrate on the folded cross dipole arms. The currents on the pair of dipole arms are opposite distributed and thus cancelled out at boresight direction.

The radiation patterns at these two null frequencies are illustrated in Figure 6. As seen, both the RHCP and LHCP levels are lower than -22 dBic, indicating satisfactory radiation suppression at these two frequencies. It is worth mentioning that since the two radiation nulls are respectively introduced by the bent mental square ring and the folded cross dipole arms, the frequencies of them can be individually controlled by tuning the corresponding length parameters.

Preprints.org (www.preprints.org) | NOT PEER-REVIEWED | Posted: 23 May 2024 doi:10.20944/preprints202405.1496.v1

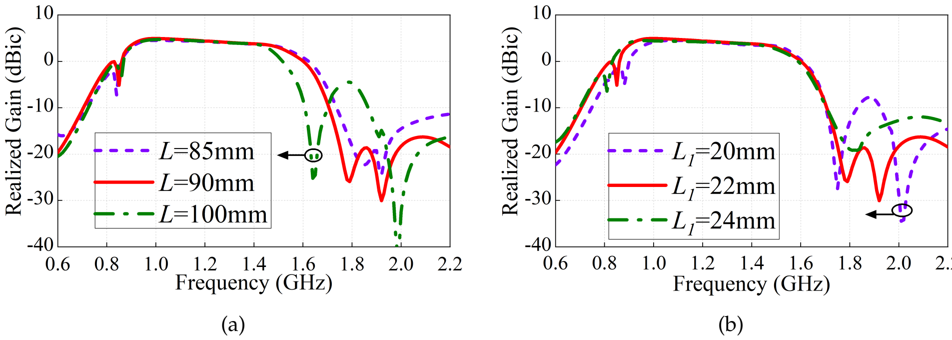

Figure 4. Frequency control of the radiation nulls at (a) 1.78 GHz and (b) 1.92 GHz.

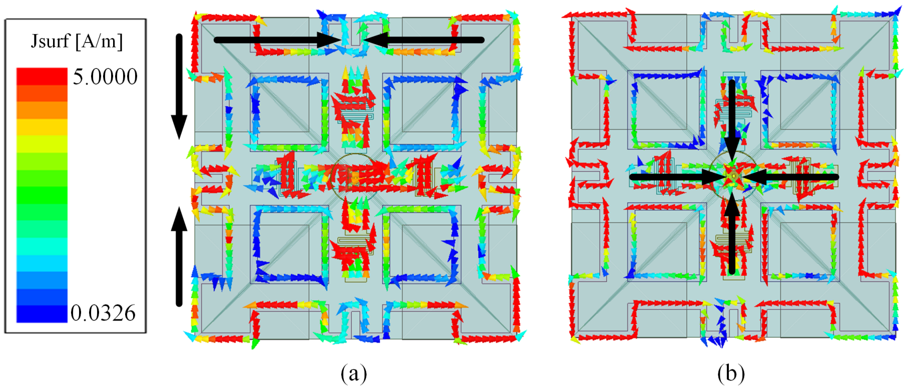

Figure 5. Current distributions on the reference Antenna V at the two null frequencies (a) $Null_1$ 1.78 GHz and (b) $Null_2$ 1.92 GHz.

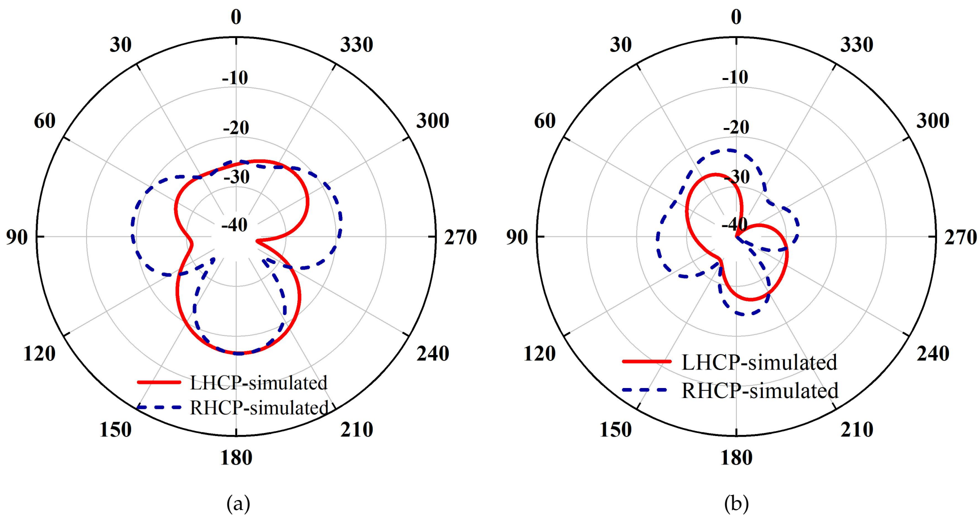

Figure 6. Simulated radiation patterns at the two null frequencies (a) 1.78 GHz and (b) 1.92 GHz.

3. Antenna Implementation

Based on the above design method, the proposed compact wideband CP cross dipole antenna with low pass filtering radiation response was designed, fabricated and measured, as shown in Figure 7(a). The optimization was performed using high frequency structural simulator (HFSS) and the

Preprints.org (www.preprints.org) | NOT PEER-REVIEWED | Posted: 23 May 2024 doi:10.20944/preprints202405.1496.v1

measurement was accomplished by Agilent N5227A network analyzer and Satimo system. The measured results including the S-parameters, realized gain and AR are shown in Figures 7(b)-(c).

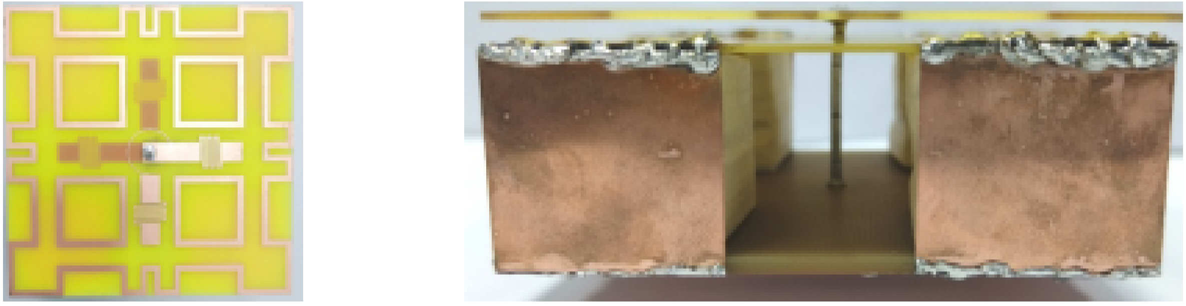

(a)

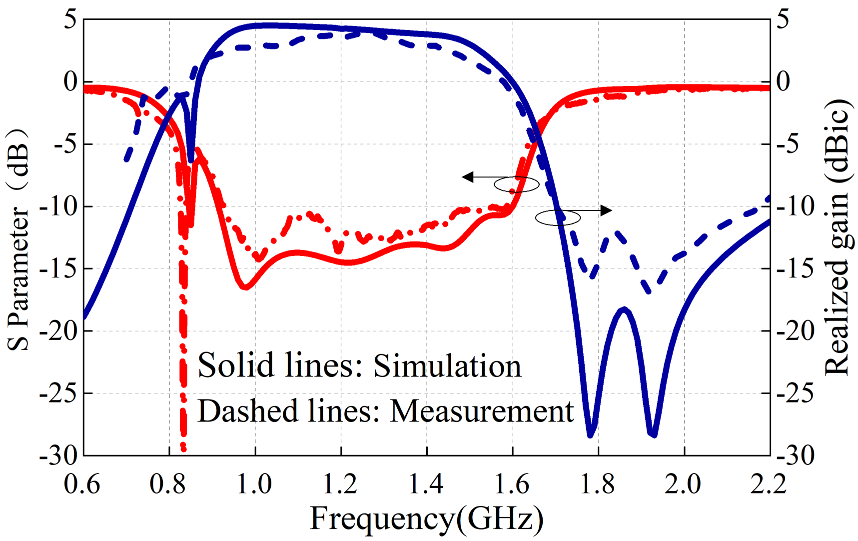

(b)

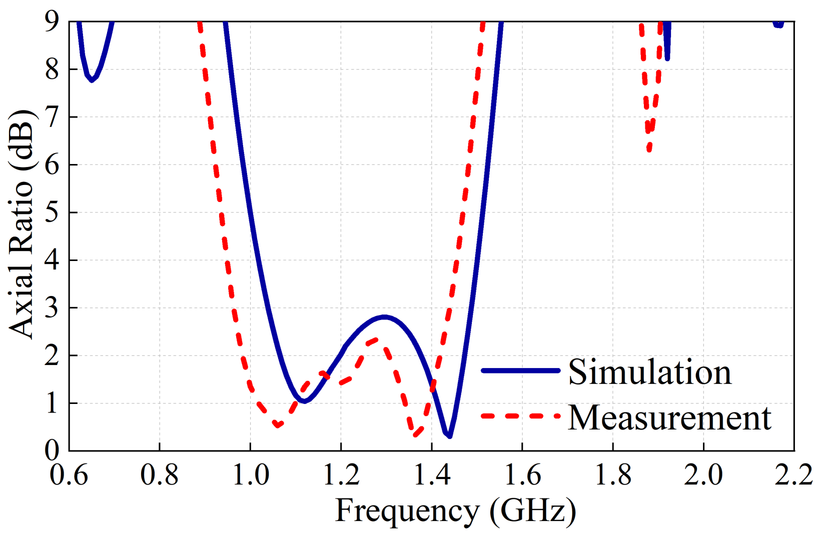

(c)

Figure 7. The proposed crossed-dipole antenna (a) Prototype, (b) measured reflection coefficients and realized gains. (c) measured ARs.

doi:10.20944/preprints202405.1496.v1

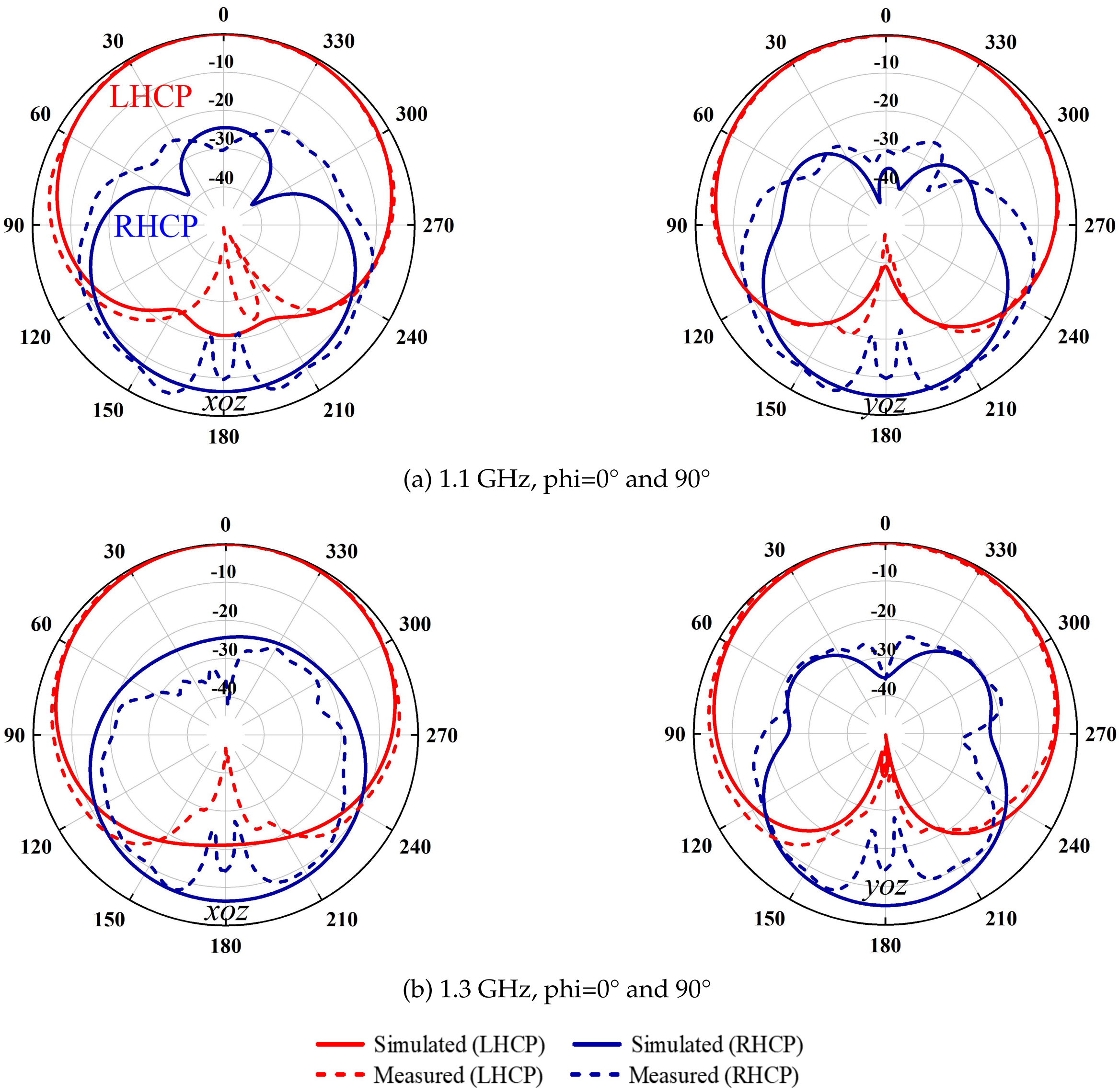

Figure 8. Radiation patterns of the proposed antenna at (a) 1.1 GHz and (b) 1.3 GHz (solid lines: simulation, dashed lines: measurement).

The simulation results agree well with the measurement ones.As seen in Figure 7(b), stable antenna LHCP realized gains about 4 dBic are obtained within the operating bandwidth. The -10 dB impedance bandwidths reach 53.3% (0.92-1.59 GHz). Two radiation nulls at about 1.78 GHz and 1.92 GHz are observed as expected, ensuring a high upper band radiation rejection level. The measured AR bandwidth is about 41% (0.95-1.44 GHz).The antenna radiation patterns at 1.1 GHz and 1.3 GHz are plotted in Figure 8. As expected, normal stable radiation patterns with low cross-polarization levels are observed. It should be mentioned that the 3dB beamwidths (HPBW) at these two frequencies are more than 120°and therefore the boresignt antenna realized gains are about 3.5-4 dBic.

To address the advantages of the proposed work, the comparison results with other related designs are tabulated in Table I. The filtering CP dipole antenna designs have been rarely proposed. In [5–10,17,19,20,22,24], the antennas have wide axial ratio bandwidths but occupied large antenna sizes or heights. In [16,18,21] folded cross dipole arms and shorted circuit radiator patch were used to realize compact CP antenna function. However, the antenna realized gains were not stable. Compared to them, the proposed work simultaneously obtained compact antenna structure $0.37\lambda_0 \times 0.37\lambda_0 \times 0.14\lambda_0$, a relatively wide axial ratio bandwidth 41%, filtering radiation response and stable in-band realized gain. In addition, the HPBW of the proposed antenna is stable about 120°. The wide HPBW and compact size make the proposed CP antenna very attractive in beam-scanning MIMO array antenna applications.

Table 1. Comparison Of The Proposed And Reported CP Cross Dipole Antennas.

	Size ($\lambda_0 \times \lambda_0$)	Height (λ_0)	Imp./AR BW (%)	Gain (dBic)	Rad. null	HPBW
[5]	0.5×0.5	0.25	60.5/31	6.1-6.9	No	68°
[6]	1.1×1.1	0.4	93.1/90.9	-2-8.6	No	N.A
[7]	0.6×0.6	0.21	98.2/85.5	4.5-10	No	N.A
[8]	0.6×0.6	0.0027	55.26/53.5	1.8-2.08	No	N.A
[9]	1.0×1.0	0.26	95.5/94.4	0-7	No	N.A
[10]	1.1×1.1	0.25	57/33	7.8-8.7	No	65°
[16]	0.2×0.3	0.0055	16.4/11.7	0.5-1.9	No	116°
[17]	0.5×0.5	0.3	40/7.3	5-6.3	No	104°
[18]	0.3×0.3	0.25	35.5/10.7	2.5-4.6	No	N.A
[19]	1.7×1.7	0.012	14.4/2.8	1.2-1.4	No	N.A
[20]	0.3×0.3	0.23	53.5/45	7.6-8.4	No	71°
[21]	0.4×0.4	0.15	92.6/71.8	-2.5-3.5	No	120°
[22]	2.4×0.7	0.16	34.6/23.1	5-8.8	No	N.A
[24]	0.6×0.6	0.16	40/19.3 49.5/33.8	4-6 4-8	No	N.A
This work	**0.37×0.37**	**0.14**	**53.3/41**	**3.5-4**	**Yes**	**120°**

4. Conclusions

In this letter, a compact wideband circularly polarized filtering dipole antenna with low-pass filtering radiation response has been proposed. The antenna has a compact antenna size due to the folded cross dipole arms and shorted circuit patches. The bent square ring and embedded four small square rings coupled to the folded cross dipole were used to obtain wideband CP performance. Lowpass-type filtering radiation response has been obtained by the bent square ring and the folded cross dipole structure to generate two specific radiation nulls at the upper band edges, without extra filter circuit. As a result, two controllable radiation nulls are generated at 1.78 GHz and 1.92 GHz, respectively, as expected.

Author Contributions: Conceptualization, X.L.; Validation, Z.W.; Software, Y.H.; Project administration, X.L.; Funding acquisition, Y.Z.; Supervision, Y.Z. All authors have read and agreed to the published version of the manuscript.

Funding: This work was supported in part by the National Natural Science Foundation of China under Grant 62001407 and Grant U2241222, in part by the College Student Innovation and Entrepreneurship Training Program Project under Grant 202311819005.(Corresponding author: Yao Zhang).

Conflicts of Interest: The authors declare no conflict of interest.

Abbreviations

The following abbreviations are used in this manuscript:

CP	Circular Polarized Antenna
AR	Axial Ratio
HPBW	Half Power Beamwidth
RHCP	Right Hand Circularly Polarized
LHCP	Left Hand Circularly Polarized
MIMO	Multi-input multi-output

References

1. Yang, W.J.; Pan, Y.M.; Zheng, S.Y. Mutual Coupling Reduction in CP MIMO Crossed-Dipole Antenna Array. *IEEE Antennas and Wireless Propagation Letters* **2022**, *21*, 2442–2446. doi:10.1109/LAWP.2022.3196371.
2. Yang, W.J.; Pan, Y.M.; Zheng, S.Y. Mutual Coupling Reduction in CP MIMO Crossed-Dipole Antenna Array. *IEEE Antennas and Wireless Propagation Letters* **2022**, *21*, 2442–2446. doi:10.1109/LAWP.2022.3196371.
3. Saurav, K.; Sarkar, D.; Srivastava, K.V. Dual-Band Circularly Polarized Cavity-Backed Crossed-Dipole Antennas. *IEEE Antennas and Wireless Propagation Letters* **2015**, *14*, 52–55. doi:10.1109/LAWP.2014.2355141.
4. He, Y.; He, W.; Wong, H. A Wideband Circularly Polarized Cross-Dipole Antenna. *IEEE Antennas and Wireless Propagation Letters* **2014**, *13*, 67–70. doi:10.1109/LAWP.2013.2296324.
5. Tu, Z.H.; Jia, K.G.; Liu, Y.Y. A Differentially Fed Wideband Circularly Polarized Antenna. *IEEE Antennas and Wireless Propagation Letters* **2018**, *17*, 861–864. doi:10.1109/LAWP.2018.2820082.
6. Feng, G.; Chen, L.; Wang, X.; Xue, X.; Shi, X. Broadband Circularly Polarized Crossed Bowtie Dipole Antenna Loaded With Parasitic Elements. *IEEE Antennas and Wireless Propagation Letters* **2018**, *17*, 114–117. doi:10.1109/LAWP.2017.2777442.
7. Feng, Y.; Li, J.; Cao, B.; Liu, J.; Yang, G.; Wei, D.J. Cavity-Backed Broadband Circularly Polarized Cross-Dipole Antenna. *IEEE Antennas and Wireless Propagation Letters* **2019**, *18*, 2681–2685. doi:10.1109/LAWP.2019.2948710.
8. Wang, H.; Byun, G.; Park, Y.B.; Park, I. Circularly Polarized Wideband Uniplanar Crossed-Dipole Antenna With Folded Striplines and Rectangular Stubs. *IEEE Access* **2023**, *11*, 63252–63260. doi:10.1109/ACCESS.2023.3289074.
9. Wang, L.; Fang, W.X.; Shao, W.H.; Yao, B.; Huang, Y.; En, Y.F. Broadband Circularly Polarized Cross-Dipole Antenna With Multiple Modes. *IEEE Access* **2020**, *8*, 66489–66494. doi:10.1109/ACCESS.2020.2981050.
10. Sefidi, M.; Ghobadi, C.; Nourinia, J.; Naderali, R. Broadband Circularly Polarized Printed Crossed-Dipole Antenna and Its Arrays for Cellular Base Stations. *IEEE Access* **2024**, *12*, 6842–6851. doi:10.1109/ACCESS.2024.3351185.
11. Mak, K.M.; Luk, K.M. A Circularly Polarized Antenna With Wide Axial Ratio Beamwidth. *IEEE Transactions on Antennas and Propagation* **2009**, *57*, 3309–3312. doi:10.1109/TAP.2009.2029370.
12. Ta, S.X.; Choo, H.; Park, I.; Ziolkowski, R.W. Multi-Band, Wide-Beam, Circularly Polarized, Crossed, Asymmetrically Barbed Dipole Antennas for GPS Applications. *IEEE Transactions on Antennas and Propagation* **2013**, *61*, 5771–5775. doi:10.1109/TAP.2013.2277915.
13. Wen, L.; Gao, S.; Luo, Q.; Hu, W.; Sanz-Izquierdo, B.; Yang, X.X. Wideband Circularly Polarized Reflectarray Antenna Using Rotational Symmetrical Crossed Dipoles. *IEEE Transactions on Antennas and Propagation* **2023**, *71*, 4576–4581. doi:10.1109/TAP.2023.3247943.
14. Tran, H.H.; Ta, S.X.; Park, I. A Compact Circularly Polarized Crossed-Dipole Antenna for an RFID Tag. *IEEE Antennas and Wireless Propagation Letters* **2015**, *14*, 674–677. doi:10.1109/LAWP.2014.2376945.
15. Lin, Y.F.; Wang, Y.K.; Chen, H.M.; Yang, Z.Z. Circularly Polarized Crossed Dipole Antenna With Phase Delay Lines for RFID Handheld Reader. *IEEE Transactions on Antennas and Propagation* **2012**, *60*, 1221–1227. doi:10.1109/TAP.2011.2180319.
16. Kedze, K.E.; Wang, H.; Kim, Y.; Park, I. Design of a Reduced-Size Crossed-Dipole Antenna. *IEEE Transactions on Antennas and Propagation* **2021**, *69*, 689–697. doi:10.1109/TAP.2020.3016392.
17. Xue, F.; Zhang, Y.; Li, J.; Liu, H. Circularly Polarized Cross-Dipole Antenna for UHF RFID Readers Applicated in the Warehouse Environment. *IEEE Access* **2023**, *11*, 38657–38664. doi:10.1109/ACCESS.2023.3253542.
18. Xu, R.; Liu, J.; Wei, K.; Hu, W.; Xing, Z.J.; Li, J.Y.; Gao, S.S. Dual-Band Circularly Polarized Antenna With Two Pairs of Crossed-Dipoles for RFID Reader. *IEEE Transactions on Antennas and Propagation* **2021**, *69*, 8194–8203. doi:10.1109/TAP.2021.3083827.
19. Inserra, D.; Wen, G. Compact Crossed Dipole Antenna With Meandered Series Power Divider for UHF RFID Tag and Handheld Reader Devices. *IEEE Transactions on Antennas and Propagation* **2019**, *67*, 4195–4199. doi:10.1109/TAP.2019.2905926.
20. Wen, L.; Gao, S.; Sanz-Izquierdo, B.; Wang, C.; Hu, W.; Ren, X.; Wu, J. Compact and Wideband Crossed Dipole Antenna Using Coupling Stub for Circular Polarization. *IEEE Transactions on Antennas and Propagation* **2022**, *70*, 27–34. doi:10.1109/TAP.2021.3090076.
21. Li, G.; Zhang, F.S. A Compact Broadband and Wide Beam Circularly Polarized Antenna With Shorted Vertical Plates. *IEEE Access* **2019**, *7*, 90916–90921. doi:10.1109/ACCESS.2019.2927284.

22. Li, L.; Zhang, C.; Shao, Y.; Luo, J. An SIW-Fed Cross-Dipole Antenna With Broadband Circular Polarization for MMW Applications. *IEEE Transactions on Antennas and Propagation* **2022**, *70*, 4830–4835. doi:10.1109/TAP.2021.3137268.
23. Ta, S.X.; Park, I. Dual-Band Low-Profile Crossed Asymmetric Dipole Antenna on Dual-Band AMC Surface. *IEEE Antennas and Wireless Propagation Letters* **2014**, *13*, 587–590. doi:10.1109/LAWP.2014.2312950.
24. Tran, H.H.; Park, I. A Dual-Wideband Circularly Polarized Antenna Using an Artificial Magnetic Conductor. *IEEE Antennas and Wireless Propagation Letters* **2016**, *15*, 950–953. doi:10.1109/LAWP.2015.2483589.